Dilutional Control of Prothrombin Activation at Physiologically Relevant Shear Rates

Laura M. Haynes,[†] Yves C. Dubief,[‡] Thomas Orfeo,[†] and Kenneth G. Mann[†*]
[†]Department of Biochemistry, University of Vermont, College of Medicine, Colchester, Vermont; and [‡]Mechanical Engineering Department, University of Vermont, College of Engineering and Mathematical Sciences, Burlington, Vermont

ABSTRACT The generation of proteolyzed prothrombin species by preassembled prothrombinase in phospholipid-coated glass capillaries was studied at physiologic shear rates (100–1000 s^{-1}). The concentration of active thrombin species (α-thrombin and meizothrombin) reaches a steady state, which varies inversely with shear rate. When corrected for shear rate, steady-state levels of active thrombin species exhibit no variation and a Michaelis-Menten analysis reveals that chemistry of this reaction is invariant between open and closed systems; collectively, these data imply that variations with shear rate arise from dilutional effects. Significantly, the major products observed include nonreactive species arising from the loss of prothrombin's phospholipid binding domain (des F1 species). A numerical model developed to investigate the spatial and temporal distribution of active thrombin species within the capillary reasonably approximates the observed output of total thrombin species at different shears; it also predicts concentrations of active thrombin species in the wall region sufficient to account for observed levels of des FI species. The predominant feedback formation of nonreactive species and high levels of the primarily anticoagulant intermediate meizothrombin (~40% of total active thrombin species) may provide a mechanism to prevent thrombus propagation downstream of a site of thrombosis or hemorrhage.

INTRODUCTION

Most of our knowledge of blood coagulation comes from experiments in closed systems. While this approach has allowed for great understanding of this important biological process (1), these studies do not reflect how the dynamics of the system may be altered in the vasculature. Several studies have looked at the activation of coagulation zymogens in purified protein systems under flow (2–9); additional studies have looked at the effect of flow on coagulation from the standpoint of modeling (10,11), as well as in whole blood and plasma-based flow experiments (11,12).

In this article, we seek to build upon previous studies investigating the activation of the zymogen prothrombin (factor (F)II) to the enzyme α-thrombin (αIIa) under conditions of flow (6,8,9). αIIa is a key enzyme in both pro- and anticoagulant pathways. The major source of αIIa is through the activation of FII by the prothrombinase complex, which is composed of factors Va and Xa (FVa-FXa), assembled on an appropriate membrane surface in the presence of calcium (Ca^{2+}). The kinetics of this process has been extensively studied in closed system experiments (1,13,14). The activation of bovine FII by membrane anchored prothrombinase is preceded by FII binding to the phospholipid membrane followed by an initial cleavage at Arg^{323} to produce meizothrombin (mIIa) and a second cleavage at Arg^{274} resulting in the generation of αIIa (15,16). A feedback cleavage at Arg^{156} of FII and mIIa by αIIa and/or mIIa results in the release of the phospholipid-binding domain, fragment 1 (F1), and the poorly reactive prethrombin-1 (Pre1) and mIIa(des F1) (17,18). A diagram of these cleavages is illustrated in Fig. S1 in the Supporting Material.

Flow contributes to a diverse number of roles in the coagulation process (19,20). In addition to its impact on cells (19), flow influences the molecular architecture of some plasma proteins such as von Willebrand Factor and ADAMTS-13 (21), provides a continuous source of substrates for the localized coagulation catalysts which form in response to vasculature damage, and removes products from the site of injury. For studies of flow within the vasculature, the wall shear rate has become an accepted means of describing localized flow conditions. Shear rates within the vasculature system cover a dynamic range from ~50 s^{-1} in the inferior vena cava to 1900 s^{-1} in the arterioles (19).

The effect of flow on a localized membrane-bound catalytic system, such as prothrombinase, is multifold. As the shear rate is increased, the rate at which new substrates are brought into the catalytically active region increases; however, the substrate residence time within that region is diminished. This creates a competition between dilutional and diffusional effects (20,22,23). In the latter instance, reaction dynamics are driven by substrate diffusion between the catalytically active wall region and the bulk solvent. Conditions favoring such dynamics include low flow rate, low substrate concentration, large tube dimensions, and low substrate diffusion constants (23).

Previous reports have investigated the influence of shear rate on product formation by prothrombinase, but in these studies the processes of prothrombinase complex formation and catalysis were not segregated (6,8,9). In this study, we examine the activation of bovine FII to αIIa and mIIa by immobilized preformed bovine prothrombinase complex at

Submitted July 14, 2010, and accepted for publication December 20, 2010.
*Correspondence: kenneth.mann@uvm.edu
Editor: Heinrich Roder.

0006-3495/11/02/0765/9 $2.00
doi: 10.1016/j.bpj.2010.12.3720

shear rates from 100 to 1000 s^{-1}, which corresponds roughly to the dynamic range of shear rates found in the arterial and much of the venous system. Additionally we investigate the enzyme kinetics of the prothrombinase complex under flow at a shear rate of 250 s^{-1}, which is representative of typical venous shear rates (19). The poorly reactive side products, mIIa(des F1) and Pre1, are quantitated and related to the distribution of active thrombin species (αIIa+mIIa) in the capillary.

Having an understanding of the complex contributions of flow to the coagulation process will permit extrapolation from test-tube experiments to more physiologically relevant open systems. This will permit an understanding of the dynamics of occlusive clot formation, and the delivery and removal of pharmaceuticals.

MATERIALS AND METHODS

Materials

Synthetic phospholipid vesicles (PCPS) were prepared from 75% dioleoyl phosphatidylcholine (PC) and 25% dioleoyl phosphatidylserine (PS) from Avanti Polar Lipids (Alabaster, AL) as described previously (24). Dansylarginine *n*-(3-ethyl-1,5-pentanediyl)amide (DAPA) (25) and Russel Viper Venom Xa Activator were gifts from Haematologic Technologies (Essex Junction, VT). Ecarin was purchased from Centerchem (Norwalk, CT). The fluorogenic FXa substrate SN-7 (26) and D-Phe-Pro-ArgCH_2Cl were prepared in house. SpectozymeTH was purchased from American Diagnostica (Stamford, CT). Heparin was purchased from Sigma-Aldrich (St. Louis, MO).

A polyclonal burro anti-human Pre1 antibody was obtained from the Antibody Core at the University of Vermont (Colchester, VT). Bovine FII, FVa, and FXa were utilized because they present a simpler system from that of their human analog and were isolated from bovine plasma (27,28) or obtained as gifts from Haematologic Technologies. Bovine FX was activated to bovine FXa with Russel Viper Venom Xa Activator. Bovine FVa was isolated as described previously, dialyzed, and stored in HBS (20 mM HEPES, 150 mM NaCl, pH = 7.4) at −80°C (29). Bovine mIIa was generated from FII using Ecarin in the presence of DAPA. Pre1 was prepared from a digestion of FII with αIIa (30) and purified using a BioCad 700E (Applied Biosystems, Foster City, CA) equipped with a HS20A column. Human antithrombin (AT) was isolated in-house (31).

Preparation of flow chamber

Borosilicate glass capillaries (2 mm × 0.2 mm × 5 cm) (Vitrocom, Mountain Lakes, NJ) were plasma-cleaned on the high setting for 30 min in a PDC-3XG plasma cleaner (Harrick, Pleasantville, NY) with atmospheric gas. Glass capillaries were filled with a solution of 100 μM PCPS vesicles in HBS2 (20 mM HEPES, 150 mM NaCl, 2 mM $CaCl_2$, pH = 7.4) and incubated at 4°C for 1 h to assemble a supported phospholipid bilayer (32,33). The capillaries were rinsed three times with HBS2 via capillary action and stored overnight under HBS2. Before each flow experiment, bovine prothrombinase was assembled in the PCPS-coated capillary at a nominal level of 4 fmoles by filling the 20 μL capillary with a solution containing 20 nM FVa and 0.2 nM FXa in HBSP2 (20 mM HEPES, 150 mM NaCl, 2 mM $CaCl_2$, 0.1% polyethylene glycol, pH = 7.4), incubating for 1 h at 37°C.

Flow experiment procedure

Temperature (37 ± 3°C) was controlled over the course of these experiments by means of a thermostat and heat lamp in an insulated Plexiglas box. Flow rates were controlled using a Model 22 syringe pump (Harvard Apparatus, Holliston, MA). A prothrombinase-coated glass capillary was attached to the pump using 23 cm of Silastic tubing (*ID* = 1.65 mm) (Dow Corning, Midland, MI) and a 20 gauge blunt tip needle. At the outflow side of the capillary 3 cm of tubing was added to ease collection. Approximately 100 μL of HBSP2 was flowed through the capillary at a shear rate of 100 s^{-1} (0.085 mL/min) before each experiment.

A reaction mixture containing FII or Pre1 in HBSP2 was flowed through the capillary at shear rates ranging from 100 to 1000 s^{-1} and collected dropwise (~23 μL/drop) into a 96-well plate with each well containing 155 μL quench buffer (20 mM HEPES, 150 mM NaCl, 20 mM EDTA, 0.1% polyethylene glycol, pH = 7.4) for analysis of αIIa+mIIa activity. The drop size was found to be consistent and independent of shear by gravitometric analysis, allowing the number of drops to be used as an internal clock. For analysis by quantitative Western blotting, two drops of effluent were collected into a final concentration of ~3.5 μM D-Phe-Pro-ArgCH_2Cl to stop further reactions.

Intrinsic fluorescence of the collected outflow was monitored to establish the time of inflowing fluid entry into the capillary using a Synergy 4 fluorescence plate reader (BioTek Instruments, Winooski, VT) at 37°C with an excitation wavelength (λ_{ex}) of 280 nm and an emission wavelength (λ_{em}) of 320 nm. SpectrozymeTH (200 μM) was used in a kinetic assay to determine the total concentration of αIIa+mIIa on a SpectraMax 340 absorbance plate reader (Molecular Devices, Sunnyvale, CA). The ratio of αIIa/mIIa in the effluent at shear rates of 250 and 500 s^{-1} was determined using the method of Côté et al. (34), which takes advantage of the differential reactivity of αIIa and mIIa toward the AT-heparin complex. Detailed descriptions of these procedures are given in the Supporting Material.

Capillary prothrombinase content was determined by removing the limiting FXa from the capillary by chelation with quench buffer (200 μL) and measuring its concentration in a fluorogenic assay (λ_{ex} = 350 nm, λ_{em} = 470 nm, cutoff filter = 450 nm at 37°C) with SN-7 (35.7 μM) in the presence of hirudin (237 nM) over 5 min on a Fluoromax-2 fluorometer (Jobin Yvon-Spex, Edison, NJ).

Steady-state concentrations of αIIa+mIIa were used in further analysis. The relative concentrations αIIa and mIIa cannot be distinguished as their reactivities toward SpectrozymeTH differ by ~10%, which is not distinguishable by the analytical techniques implemented (35,36). Quantitative Western blotting was used to estimate the extent of αIIa+mIIa diffusion from the rate of des F1 species generation as described in the Supporting Material.

Closed system kinetic analyses

The rates of FII activation by prothrombinase and FII conversion to Pre1 by αIIa+mIIa in closed systems were determined as described in the Supporting Material.

THEORY

A numerical model for the activation of FII to αIIa based on a one-step mechanism is used to gain insights into the spatial distribution of αIIa+mIIa that cannot be measured experimentally and to synthesize our findings. This model does not include the feedback cleavage at Arg^{156} (for justification, see Supporting Material) and solves for the transport of αIIa+mIIa in a fully developed, two-dimensional channel flow. The dimensions of the channel match the height (*H*) and length (*L*) of the experimental capillary. The flow and species transport is characterized by the Reynolds number,

$$Re_b = U_b h/\nu,$$

and, for each species (here denoted by i), the Peclet number

$$Pe_i = U_b h/D_i,$$

and the Schmidt number

$$Sc_i = \nu/D_i,$$

where U_b is the bulk velocity, ν the solvent viscosity, h is the half-height of the capillary, and D_i the diffusivity of species i. The Reynolds and Peclet numbers are the ratio of inertia to viscous forces in the solvent and the inertia to species diffusivity, respectively. Lastly, the reaction rate is characterized by the Damköhler number

$$Da_i = k_{cat} h^2/D_i,$$

the ratio of the chemical reaction rate to diffusion rate. These parameters are listed in Table 1.

The low Reynolds and the large Peclet numbers indicate that the flow is laminar and that the transport of species is dominated by flow convection. The relatively large Damköhler number also indicates that the activation of FII under these flow conditions is dominated by the reaction rate. Due to the low Reynolds number of the flow and a smooth junction between the tube connecting to the capillary to the pump, it is assumed that the flow in the capillary is fully developed and the effect of side walls is negligible. The capillary is therefore modeled in a two-dimensional domain where the velocity profile is defined as the Poiseuille velocity profile,

$$u(z) = Sz\left(1 - \frac{z}{H}\right), \quad (1)$$

where z is the vertical coordinate and S the wall shear of the flow. FII activation is modeled by a one-step reaction in which αIIa and mIIa are treated as equivalently active species,

$$\text{FII} \xrightarrow{\text{prothrombinase}} (\alpha\text{IIa} + \text{mIIa}), \quad (2)$$

which occurs within a thin shell at the capillary walls under Michaelis-Menten kinetics defined by empirical constants obtained under flow conditions at 250 s^{-1} in this study. The model differs from Neeves et al. (2), where the reaction is considered to take place on the surface of the channel. Although the two methods are equivalent, our motivation for the shell model is to test the proposition (37) that FII activation may be modeled as occurring in a 8.5-nm shell volume around vesicle outer membranes in a static system. The reaction is therefore present in the transport equation of species, φ, as source term Π_φ (φ = FII or αIIa+mIIa),

$$u(z)\frac{\partial \varphi}{\partial x} = D_\phi\left(\frac{\partial^2 \varphi}{\partial x^2} + \frac{\partial^2 \varphi}{\partial z^2}\right) + \prod_\varphi, \quad (3)$$

where x is the longitudinal direction, and D_φ is the diffusivity coefficient of φ. The inlet concentration of FII (1.4 μM) is constant. The source term is zero everywhere except for $z \le \Delta$ or $(H-z) \le \Delta$ and $x \ge 0$, with $\Delta = 8.5$ nm, where $\Pi_{\text{II}} = -V$ and $\Pi_{\alpha\text{IIa+mIIa}} = +V$, where V is the rate of the reaction. Equation 3 is solved using an in-house computational fluid dynamics code, described in the Supporting Material along with grid convergence studies. The computational domain is defined between -1 cm $\le x \le 5$ cm and $0 \le z \le 0.2$ mm. Simulations are run to steady-state convergence, inasmuch as this study is only interested in the steady-state production of αIIa+mIIa. The concentration of product at any location x is calculated from its mass flux,

$$\overline{[\alpha IIa + mIIa]}_x = \frac{6}{SH^2}\int_0^H [\alpha IIa + mIIa](x,z)\, u(z)\, dz, \quad (4)$$

where $u(z)$ is the flow velocity defined in Eq. 2 and $SH^2/6$ is the flux of fluid per unit width in the capillary. Equation 4 is used with $x = L$ for the simulated concentration of product at the end of the capillary.

The dilutional effect on FII activation is easily predicted by considering that Eq. 3 is similar to the well-known Graetz problem (38), which yields a self-similar solution in the form

$$[\alpha IIa + mIIa] = [\alpha IIa + mIIa]_w(x) \cdot f(\eta), \quad (5)$$

where $[\alpha\text{IIa+mIIa}]_w(x)$ is the wall concentration at a distance x from the onset of activation. The vertical coordinate is normalized by the concentration boundary layer thickness,

$$\eta = \frac{z}{\delta_{FIIa}(x)}. \quad (6)$$

The concentration boundary layer thickness is typically defined as the local altitude at which the concentration is, in the case of αIIa+mIIa, a fixed fraction of a reference concentration. Here, the edge of the concentration boundary layer may actually be defined by the critical threshold of αIIa+mIIa (2 nM) to cause clot formation (39). Considering that the transport mechanisms of αIIa and mIIa are only a function of shear and diffusion (Eq. 3), the growth of the concentration boundary layer may be estimated from dimensional considerations with the diffusion coefficients (D) listed in Table 1. The $D_{\alpha\text{IIa}}$ was used to model both αIIa and mIIa diffusion, as

TABLE 1 Relevant constants and fluid dynamics terms at 37°C

Parameter	Value
Reynolds number	1–10
Peclet number	10^4–10^5
Damköhler number	8000
D_{FII}*	9.35×10^{-11} m^2 s^{-1}
$D_{\alpha\text{IIa}}$†	13.42×10^{-11} m^2 s^{-1}

*From Lim et al. (50).
†From Harmison et al. (51).

$$\delta_{FIIa}(x) \propto \left(\frac{D_{\alpha IIa}x}{S}\right)^{1/2}. \quad (7)$$

Using conservation of concentration over a control volume between x and $x+\Delta x$, the argument can be made (see the Supporting Material) that the wall concentration of αIIa and mIIa increases linearly with the boundary layer concentration,

$$[FIIa + mIIa]_w(x) \approx C\delta_{FIIa+mIIa}(x), \quad (8)$$

where C is a constant of units $M\ m^{-1}$. Combining Eqs. 5–8 into Eq. 4, the concentration of αIIa + mIIa collected at any location x, $\overline{[\alpha IIa + mIIa]}_x$, may be estimated as

$$\overline{[\alpha IIa + mIIa]}_x \approx 12C\frac{D_{\alpha IIa}x}{SH^2}\int_0^1 \eta\left(1 - \frac{\delta_{\alpha IIa+mIIa}(x)}{H}\eta\right)f(\eta)d\eta. \quad (9)$$

When

$$\delta_{FIIa} + {}_{mIIa}(x) \ll H,$$

the integral in Eq. 9 reduces to

$$\int_0^1 \eta f(\eta)d\eta,$$

which is independent of shear, and the product is therefore proportional to

$$\overline{[\alpha IIa + mIIa]}_x \propto x/S. \quad (10)$$

This assumption proves to be valid for $x = L$ even at the lowest shear, for which the product boundary layer merges toward the end of the capillary. A boundary layer thickness based on 2 nM of αIIa+mIIa is, from the perspective of Eq. 10, only valid in the immediate downstream vicinity of the onset of FII activation. In vivo prothrombinase activity is confined to relatively small regions, thus our initial definition of the concentration boundary layer thickness is relevant. Our empirical model, however, requires a modification to include the integrated effect of prothrombinase over a relatively larger region—an effective boundary layer thickness that accounts for the competition between flow and αIIa+mIIa diffusion. A more adequate approach to model our empirical system is to consider a normalization of the distance from the wall by the left-hand side of Eq. 7, i.e.,

$$\eta = z/\delta_D(x),$$

where

$$\delta_D(x) = (D_{\alpha IIa}x/S)^{1/3}.$$

This boundary layer definition, similar to that used by Neeves et al. (2), yields $\delta_D(L)/H \leq 0.4$ for the lowest shear. The effective boundary layers developing over the top and lower wall do not merged at the end of the capillary at low shear. Moreover, $\delta_D(L)/H << 1$ is verified over most of the capillary length (see the Supporting Material), which results in the linear dependence of αIIa+mIIa in x.

RESULTS

Determination of total prothrombinase in capillaries

Twenty-seven capillaries used in this study were analyzed for their respective FXa contents and were determined to contain 3.9 ± 1.9 fmoles (standard deviation). Despite the large standard deviation, this number is in agreement with the theoretical 4 fmoles of FXa introduced to the capillary, suggesting the prothrombinase is not being eluted from the capillary. Variations in FXa levels did not correlate with variations in amounts of αIIa+mIIa generated in a given capillary.

Active thrombin species generation under flow

Typical FII (1.4 μM) activation curves are shown in Fig. S5 across the range of shear rates in this study (100–1000 s^{-1}). The absolute steady-state levels of αIIa+mIIa show a decrease with increasing shear rate (Fig. 1). When αIIa+mIIa concentrations are adjusted for the effective volumetric dilution due to increasing shear rate, the normalized αIIa+mIIa concentrations at the steady state appear nearly equivalent (Fig. 1, *inset*). Deviations in FII activation observed at higher shear rates (750 and 1000 s^{-1}) within the empirical data are not statistically significant from lower shear rates due to detection limits of the assay and shear-induced dilutional effects. To overcome these limitations,

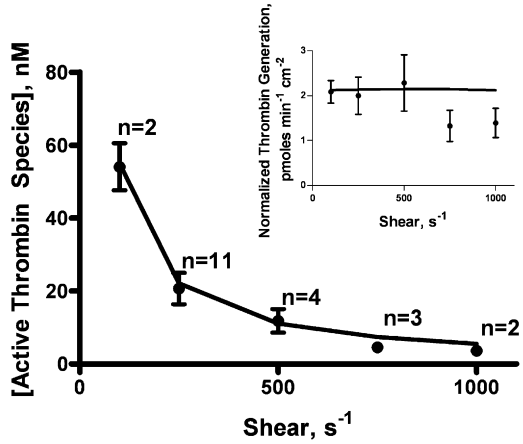

FIGURE 1 Steady-state concentrations of active thrombin species across physiologic shear rates. Steady-state levels of αIIa+mIIa generation at shear rates between 100 and 1000 s^{-1} are shown as the average and the standard deviation of repeated measurements as denoted by n. Note the decrease in the absolute concentration of active thrombin species with increasing shear rate. When normalized to account for shear rate and prothrombinase density (*inset*), the generation of active thrombin species is consistent across the range of shear rates. Empirical results are compared to our computational model (*solid lines*).

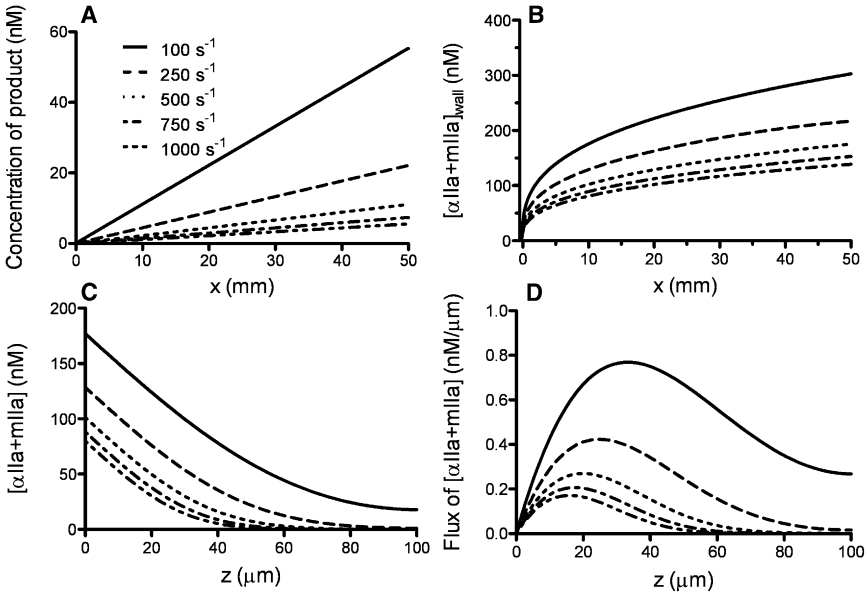

FIGURE 2 Computational models of FII activation of under flow. (*A*) Linear dependence of total αIIa+mIIa concentration on the streamwise distance from the entrance of the capillary, *x*, as a function of shear rate (100–1000 s^{-1}) as indicated in the legend. (*B*) The concentration of αIIa+mIIa as a function of *x* in the wall region ($[\alpha FIIa+mIIa]_{wall}$), defined at a height of 8.5 nM. (*C*) αIIa+mIIa concentration profiles in the vertical direction at the capillary exit as a function of shear rate. (*D*) αIIa+mIIa flux profiles in the vertical direction at the capillary exit as a function of shear rate. For panels *C* and *D*, only the lower half of the capillary is plotted.

experiments were performed at 2.5-times more prothrombinase. These also exhibited no statistically significant change in steady-state αIIa+mIIa levels when shear rate corrected (data not shown). Fig. 1 also displays the good agreement between the computational model and empirical measurements and validates the 1/S behavior described in Eq. 7.

Fig. 2 presents computational analyses detailing the shear dependence of the distribution of αIIa+mIIa as a function of distance along the capillary (Fig. 2, *A* and *B*) and from the catalytically active wall (Fig. 2, *C* and *D*). Consistent with the empirical data, the computational model shows an inverse dependence between shear and αIIa+mIIa levels across the capillary (Fig. 2 *A*), as well as in the shell region, defined as 8.5 nM above the capillary wall (Fig. 2 *B*). However, αIIa+mIIa levels in the wall region are less sensitive to shear, showing only a 2.5-fold variation versus the 10-fold range over the total cross section. The distribution of αIIa+mIIa at the exit of the capillary is illustrated spatially (Fig. 2 *C*) and with respect to product flux (Fig. 2 *D*). Significant diffusion away from the wall region is notable at lower shear rates, indicating that transport of products away from the wall will be most extensive with reduced flow.

Michaelis-Menten analysis of FII activation under flow

The steady-state levels of αIIa+mIIa as a function of FII concentration were studied at a shear rate of 250 s^{-1} (Fig. 3). At the steady-state plateau, the rate of reaction (V_{rxn}) is equivalent to the initial rate in a closed system because of the constant influx of substrate. V_{rxn} was determined by taking the absolute αIIa+mIIa concentration at the steady state and dividing it by the average time it takes one capillary volume to transit the capillary (5.6 s at a shear rate of 250 s^{-1}). The concentration of enzyme was assumed to be 200 pM (the nominal 4 fmoles of limiting FXa in the 20 μL capillary). From these measurements, a Michaelis-Menten analysis was conducted (Fig. 3). Under flow conditions at 250 s^{-1} and 37°C, the kinetic constants were determined to be $K_m = 0.16 \pm 0.1$ μM and $k_{cat} = 27 \pm 4\ s^{-1}$. A closed system Michaelis-Menten analysis of this reaction using the same reagents at 37°C showed similar kinetic constants compared to the flow system ($K_m = 0.24 \pm 0.1$ μM and $k_{cat} = 25 \pm 3\ s^{-1}$) and in close agreement with literature values (40).

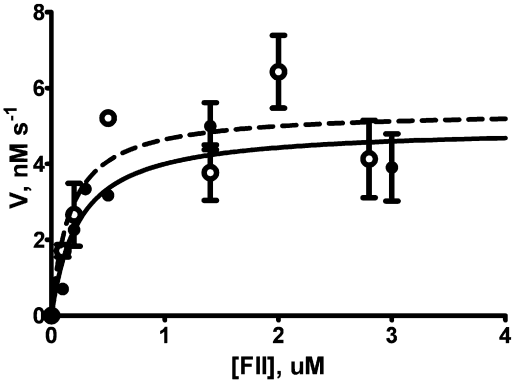

FIGURE 3 Kinetic analysis of FII activation by preassembled prothrombinase under flow. The rate of FII activation to active thrombin species is shown here as a function of prothrombin concentration in the inflowing fluid at a shear rate of 250 s^{-1}. The open circles (○) represent measured values and error bars show the standard deviation of a least two measurements. (*Dotted line*) Fit of the data to the Michaelis-Menten equation. From this fit, kinetic constants were obtained which are in close agreement with those obtained in closed system experiments shown in the solid circles (●).

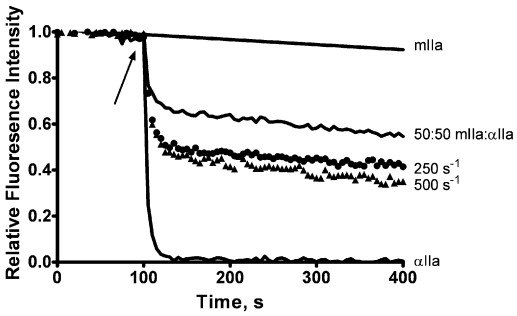

FIGURE 4 Identification of active thrombin species produced under flow. Inflowing fluid containing 1.4 μM FII was flowed over phospholipid-coated capillaries containing a nominal 4 fmoles assembled prothrombinase and collected into 500 nM DAPA to a final volume of 2 mL. AT (1 μM) was added ($t = 0$) and incubated at 25°C while monitoring the fluorescence signal ($\lambda_{ex} = 280$ nm, $\lambda_{em} = 565$ nm). Heparin (6 units mL^{-1}) was added (*arrow*) after 100 s and the fluorescence signal was recorded for an additional 300 s. The percent decline in fluorescence intensity relative to that of the collected effluent in the presence of DAPA and AT corresponds to the relative ratio of mIIa to αIIa. The ratios of mIIa/αIIa at a shear rate of 250 s^{-1} (•) and 500 s^{-1} (▲) are shown. Curves indicating control experiments with 100% mIIa, 100% FIIa, and a 50:50 mixture are also shown as indicated.

Ratio of mIIa/αIIa generation under flow

To distinguish the amount of the catalytically active intermediate mIIa present in the effluent, we utilized the differential reactivities of mIIa and αIIa toward AT and heparin. It has been reported previously that while αIIa and mIIa are both inhibited by AT, the presence of heparin dramatically increases AT inhibition of αIIa but not of mIIa or mIIa(des F1). This reaction can be monitored by displacement of DAPA (34) from the enzyme-DAPA complex. Fig. 4 illustrates representative results of this assay at 250 and 500 s^{-1}. The ratio of αIIa/mIIa was 3:2 independent of shear at these flow rates. See Table 2 for information on the relative activity of meizothrombin.

Generation of des F1 species under flow and estimates of active thrombin species concentrations

αIIa and mIIa cleave FII and mIIa at Arg^{156}, removing the membrane binding F1 domain from and resulting in Pre1 and mIIa(des F1), respectively. This cleavage reduces the effective concentration of FII because Pre1 and mIIa(des F1) have lost their membrane binding domains. The Western blot of nonreduced samples obtained at a shear rate of 250 s^{-1} in Fig. 5 *A* shows modest but significant amounts of des F1 species (Pre1 and mIIa(des F1)) being generated. The concentration of des F1 products permits estimation of the localized αIIa+mIIa, which is ~2.9 times the concentration of αIIa observed in the collected effluent between 49 and 204 s. The relative distribution of des F1 species and αIIa are fairly consistent across this time-frame, with the average of two experiments showing this ratio to be 2.3 ± 0.9. The time-course of αIIa generation estimated from densitometry in this analysis is consistent with activity measurements of αIIa+mIIa in the effluent (Fig. 5 *B*). Overall, ~96% of the FII is not proteolyzed, with ~3% des F1 species (Pre1 ≥ 2.5%), 1% αIIa, and 0.5% mIIa and mIIa (des F1) being generated under steady-state conditions. The computational model provides a spatial and temporal justification for the high levels of des F1 species observed.

The second-order rate constant for αIIa proteolysis at Arg^{156} resulting in Pre1 formation in the presence of 2 mM Ca^{2+} and 20 μM PCPS was determined under closed

TABLE 2 Relative activity of meizothrombin

Substrate	Relative activity (% αIIa)*
Fibrinogen	7%
Platelets	2%
Thrombomodulin + Protein C	93%
Thrombomodulin + TAFI†	10%

*From Côté et al. (34).
†Thrombin activatable fibrinolysis inhibitor.

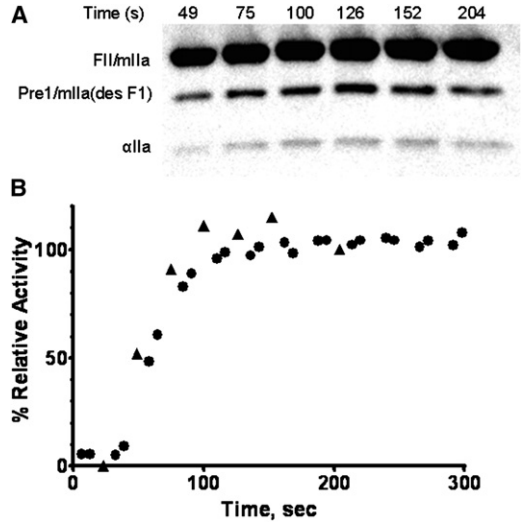

FIGURE 5 Feedback production of des F1 species under flow. (A) Representative nonreduced Western blot of reaction products formed when 1.4 μM FII is flowed through a phospholipid-coated capillary containing a nominal 4 fmoles prothrombinase at a shear rate of 250 s^{-1}. Effluent (two drops) was collected into D-Phe-Pro-ArgCH_2Cl (~32 μM) and analyzed by sodium dodecyl sulfate-polyacrylamide gel electrophoresis gel electrophoresis using a 4–12% gradient gel before transfer to a nitrocellulose membrane. The membrane was probed with a burro anti-human pre1 polyclonal antibody. Species are labeled on the left and the time course under flow is indicated above each lane. The intense FII band indicates that only a small fraction of the bulk FII in the inflowing fluid is being consumed (<5%) under flow, in agreement with thrombin activity assays (Figs. 1 and 2). The mIIa formation accounts for ~0.5% of the initial FII concentration. (*B*) Typical thrombin generation profile at a shear rate of 250 s^{-1} with an initial FII concentration of 1.4 μM in the inflowing fluid in the solid circles (•). The solid triangles (▲) show relative αIIa generation from the nonreduced Western blot in panel *A* where αIIa generation at 204 s was taken to be 100%.

system conditions to be 7000 M^{-1} s^{-1}—comparable with previously reported literature values (17,18). Given the ratio of αIIa to Pre1 determined by Western blot analysis, the concentrations of αIIa+mIIa in the wall region must be at least an order-of-magnitude higher than those measured in the bulk effluent. This observation is in agreement with our computational model (Fig. 2 *B*), which predicts that the concentration of αIIa+mIIa in the wall region is relatively undiluted by diffusional processes and at a level sufficient to catalyze the formation of these prothrombin cleavage products.

Pre1 activation under flow

With Pre1 as the initial substrate over a capillary, little generation of αIIa+mIIa was observed as compared to FII at the same concentration and shear rate (Fig. 6). Given the low concentrations of αIIa+mIIa generated in the Pre1 system, we were unable to quantify the types of species being formed. These results indicate that in the absence of the phospholipid binding domain there is limited activation of Pre1 relative to FII, consistent with the conclusion that the substrate is delivered to the enzyme by the membrane (42).

DISCUSSION

When normalized for flow dilution, αIIa+mIIa levels at steady state are constant over the shear rates in this study. This observation is consistent with the conclusion that decreases in αIIa+mIIa in the outflow are a direct result of a dilutional effect corresponding to the time that a given volume of fluid spends in the catalytically active capillary. From this perspective, a model can be devised in which

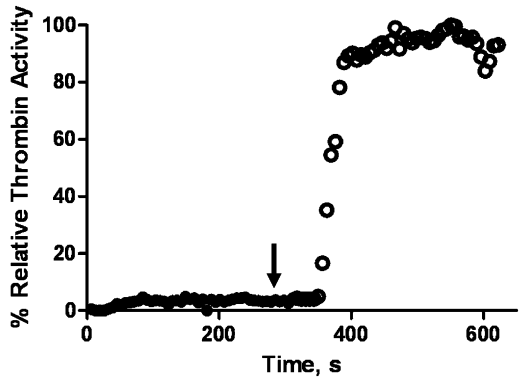

FIGURE 6 Activation of Pre1 under flow. Inflowing fluid containing 1.4 μM Pre1 was flowed through a phospholipid-coated capillary containing a nominal level of 4 fmoles prothrombinase and the effluent was assayed for thrombin activity (•). Subsequently the same capillary was perfused with an inflowing fluid containing 1.4 μM FII at ~300 s (*arrow*) and assayed for thrombin activity (○). The concentration of active thrombin species is presented as a percentage relative to the greatest concentration of thrombin measured.

the zymogens in the flowing fluid will have less time to diffuse to the catalytic factories on the capillary surface as the shear rate is increased. The implication of this observation is that it is the intrinsic differences in shear rates throughout the vasculature that are, at least partially, responsible for the regulation of coagulation. Variations in the local αIIa+mIIa concentrations under changing flow conditions (Fig. 2) most likely serve to drive different mechanisms of clot formation (2,43), while the chemistry of FII activation is independent of flow (Figs. 1 (*inset*) and 4).

The relatively high physiologic concentration of FII provides an abundant source of potential substrate and prevents depletion of substrate that can diffuse to the catalytically active wall (22,23). This level of regulation ensures that FII activation follows the same biochemistry regardless of where in the vasculature it is taking place; however, the physiologic outcome may be different because of shear-rate-dependent volumetric dilution. Regions of high shear may be less prone to fibrin clot formation than those of low shear because of the decreased time a given volume of reactant fluid spends in the catalytically active region. This correspondence has been classically suggested by Virchow (44), as well as more recently in empirical work by Neeves et al. (2). Observations of pathological differences between venous and arterial clots also support this conclusion (43). Low-shear venous, red clots predominantly consist of a fibrin network, whereas high-shear arterial, white clots consist primarily of platelets stabilized by fibrin. These differences are presumably due to the rates at which the fibrin networks are formed—in venous thrombosis lower shear rates allow for the accumulation of red blood cells within the clot.

The Michaelis-Menten analysis of the plateau levels of αIIa+mIIa generation at a shear rate of 250 s^{-1} is in good agreement with closed system experiments conducted with the same reagents. Given the steady-state conditions for which measurements under flow were obtained, it can be assumed that equilibrium conditions between FII and the membrane have been achieved and are therefore not included in our theoretical model. Additionally, FII activation by prothrombinase is a complex process, in which a catalytically active intermediate is treated as a product with regard to initial rate determination. Our theoretical model mirrors this well-established practice and utilizes a one-step process for total αIIa+mIIa generation (14,25) as reflected in the Michaelis-Menten constants. Correspondence between our model and empirical measurements confirms that observations made at 250 s^{-1} can be extrapolated to other physiologically relevant shear rates.

Our modeling confirms that while diffusion within the wall region is important, there is little diffusion away for the wall of αIIa+mIIa on the timescale of these reactions (Fig. 3). This supports a model in which dilution is the major physical force governing the dynamics of these reactions. During thrombosis, αIIa+mIIa can only exist in a relatively

small region close to the vessel walls, a hypothesis that has been previously put forth in numerical modeling studies of coagulation under flow (10) and is supported by our computational model—especially at increasing shear rates. This reduced volume element leads to increased localized concentrations of species where the reactive catalysts are bound to the surface of the vasculature. It can be surmised that concentrations of active clotting factors measured in whole samples do not accurately represent those in the actual region of physiologic clot formation, which can be an order-of-magnitude higher than those observed in the bulk solution; thus, the ability of αIIa+mIIa to drive numerous localized reactions is greatly increased due to flow dynamics and needs to be considered in both hemostatic and thrombotic pathologies.

In this work, the formation of functionally compromised des F1 species confirms the model predictions of spatially constrained surface-derived products under flow. Although AT is present under normal physiologic conditions and will suppress the levels of αIIa+mIIa, we propose that the formation of des F1 species may be a physiologically important process because the second-order rate constants for AT inhibition of αIIa+mIIa and des F1 species formation by αIIa+mIIa are of the same order of magnitude (47,48). The formation of des F1 species will lead to a negative feedback system for shutting down the coagulation process and preventing further thrombus formation downstream of the original injury site. While we do not model the formation of des F1 species (observed to be ~3% of initial FII concentration) directly, these concentrations are not surprising given the given the high localized concentrations of αIIa+mIIa observed in our model combined with the long residence time of fluid in the wall region under laminar flow.

A unique aspect of studying prothrombinase under flow is that it permits the detection of both αIIa and mIIa because a fraction of the intermediate mIIa is removed from the capillary and prevented from fully reacting. The observed ratio of mIIa/αIIa is similar to that previously reported (6). The presence of the large proportion of mIIa in the reaction effluent is consistent with closed system evidence that the reaction proceeds via a two-step mechanism in which the zymogen FII is first converted, by cleavage at Arg^{323}, to the active intermediate mIIa before being released from a first prothrombinase encounter site to seek out a second catalytic site where it is fully converted to αIIa (14).

The failure to convert all of the reacting FII to αIIa that was observed under flow effectively alters the procoagulant properties of this system. mIIa has been previously identified as an intermediate of FII activation in whole blood (49), and although it exhibits similar enzymatic activity as αIIa toward small molecule substrates, there are several important differences in substrate preference with physiologic significance. mIIa has greatly reduced activity toward platelets and fibrinogen relative to αIIa, and thus is comprised in its procoagulant function.

In addition, when the two thrombin species are compared in complex with thrombomodulin (TM), the mIIa-TM complex is relatively inefficient in activating thrombin-activatable fibrinolysis inhibitor which functions to help stabilize the fibrin clot, while the mIIa-TM complex maintains its ability to activate protein C leading to the inactivation of FVa (34,36). Thus, αIIa serves primarily a procoagulant function, while mIIa serves an anticoagulant function (Table 2). The large proportion of mIIa predicted by this model can be swept downstream of the catalytic region where it may serve to minimize thrombus formation in addition to the accumulation of poorly reactive des F1 species.

SUPPORTING MATERIAL

Additional methods, five figures, and one table are available at http://www.biophysj.org/biophysj/supplemental/S0006-3495(10)05293-8.

The authors thank Bradford Elmer and Matthew Whelihan for their technical assistance and Dr. Michael Nesheim for helpful discussions. We also thank Dr. Saulius Butenas for synthesizing the SN-7 fluorogenic substrate.

This work was supported by grant No. P01HL46703 (project 1) from the National Institutes of Health. L.M.H. is supported by a Hemostasis and Thrombosis Training Grant No. 5T32HL007594 from the National Heart, Lung and Blood Institute. Y.C.D. acknowledges the computational support of the Vermont Advanced Computing Center. K.G.M. is chairman of the board of Haematologic Technologies Inc.

REFERENCES

1. Mann, K. G., M. E. Nesheim, …, S. Krishnaswamy. 1990. Surface-dependent reactions of the vitamin K-dependent enzyme complexes. *Blood.* 76:1–16.
2. Neeves, K. B., D. A. Illing, and S. L. Diamond. 2010. Thrombin flux and wall shear rate regulate fibrin fiber deposition state during polymerization under flow. *Biophys. J.* 98:1344–1352.
3. Gemmell, C. H., V. T. Turitto, and Y. Nemerson. 1988. Flow as a regulator of the activation of factor X by tissue factor. *Blood.* 72:1404–1406.
4. Contino, P. B., H. A. Andree, and Y. Nemerson. 1994. Flow dependence of factor X activation by tissue factor-factor VIIa. *J. Physiol. Pharmacol.* 45:81–90.
5. Andree, H. A., P. B. Contino, …, Y. Nemerson. 1994. Transport rate limited catalysis on macroscopic surfaces: the activation of factor X in a continuous flow enzyme reactor. *Biochemistry.* 33:4368–4374.
6. Schoen, P., T. Lindhout, …, H. C. Hemker. 1990. Continuous flow and the prothrombinase-catalyzed activation of prothrombin. *Thromb. Haemost.* 64:542–547.
7. Gemmell, C. H., Y. Nemerson, and V. Turitto. 1990. The effects of shear rate on the enzymatic activity of the tissue factor-factor VIIa complex. *Microvasc. Res.* 40:327–340.
8. Billy, D., H. Speijer, …, T. Lindhout. 1995. Prothrombin activation by prothrombinase in a tubular flow reactor. *J. Biol. Chem.* 270:1029–1034.
9. Schoen, P., and T. Lindhout. 1991. Flow and the inhibition of prothrombinase by antithrombin III and heparin. *Blood.* 78:118–124.
10. Fogelson, A. L., and N. Tania. 2005. Coagulation under flow: the influence of flow-mediated transport on the initiation and inhibition of coagulation. *Pathophysiol. Haemost. Thromb.* 34:91–108.

11. Runyon, M. K., C. J. Kastrup, …, R. F. Ismagilov. 2008. Effects of shear rate on propagation of blood clotting determined using microfluidics and numerical simulations. *J. Am. Chem. Soc.* 130:3458–3464.
12. Shen, F., C. J. Kastrup, …, R. F. Ismagilov. 2008. Threshold response of initiation of blood coagulation by tissue factor in patterned microfluidic capillaries is controlled by shear rate. *Arterioscler. Thromb. Vasc. Biol.* 28:2035–2041.
13. Mann, K. G., R. J. Jenny, and S. Krishnaswamy. 1988. Cofactor proteins in the assembly and expression of blood clotting enzyme complexes. *Annu. Rev. Biochem.* 57:915–956.
14. Krishnaswamy, S., K. G. Mann, and M. E. Nesheim. 1986. The prothrombinase-catalyzed activation of prothrombin proceeds through the intermediate meizothrombin in an ordered, sequential reaction. *J. Biol. Chem.* 261:8977–8984.
15. Nesheim, M. E., and K. G. Mann. 1983. The kinetics and cofactor dependence of the two cleavages involved in prothrombin activation. *J. Biol. Chem.* 258:5386–5391.
16. Krishnaswamy, S., W. R. Church, …, K. G. Mann. 1987. Activation of human prothrombin by human prothrombinase. Influence of factor Va on the reaction mechanism. *J. Biol. Chem.* 262:3291–3299.
17. Petrovan, R. J., J. W. Govers-Riemslag, …, J. Rosing. 1998. Autocatalytic peptide bond cleavages in prothrombin and meizothrombin. *Biochemistry.* 37:1185–1191.
18. Silverberg, S. A. 1979. Proteolysis of prothrombin by thrombin. Determination of kinetic parameters, and demonstration and characterization of an unusual inhibition by Ca^{2+} ions. *J. Biol. Chem.* 254:88–94.
19. Hathcock, J. J. 2006. Flow effects on coagulation and thrombosis. *Arterioscler. Thromb. Vasc. Biol.* 26:1729–1737.
20. Nemerson, Y., and V. T. Turitto. 1991. The effect of flow on hemostasis and thrombosis. *Thromb. Haemost.* 66:272–276.
21. Reininger, A. J. 2008. Function of von Willebrand factor in hemostasis and thrombosis. *Haemophilia.* 14 (*Suppl 5*):11–26.
22. Koyayashi, T., and K. J. Laidler. 1974. Theory of the kinetics of reactions catalyzed by enzymes attached to the interior surfaces of tubes. *Biotechnol. Bioeng.* 16:99–118.
23. Laidler, K. J., and P. S. Bunting. 1980. The kinetics of immobilized enzyme systems. *Methods Enzymol.* 64:227–248.
24. Higgins, D. L., and K. G. Mann. 1983. The interaction of bovine factor V and factor V-derived peptides with phospholipid vesicles. *J. Biol. Chem.* 258:6503–6508.
25. Nesheim, M. E., F. G. Prendergast, and K. G. Mann. 1979. Interactions of a fluorescent active-site-directed inhibitor of thrombin: dansylarginine *n*-(3-ethyl-1,5-pentanediyl)amide. *Biochemistry.* 18:996–1003.
26. Butenas, S., T. Orfeo, …, K. G. Mann. 1992. Aminonaphthalenesulfonamides, a new class of modifiable fluorescent detecting groups and their use in substrates for serine protease enzymes. *Biochemistry.* 31:5399–5411.
27. Bajaj, S. P., and K. G. Mann. 1973. Simultaneous purification of bovine prothrombin and factor X. Activation of prothrombin by trypsin-activated factor X. *J. Biol. Chem.* 248:7729–7741.
28. Nesheim, M. E., K. H. Myrmel, …, K. G. Mann. 1979. Isolation and characterization of single chain bovine factor V. *J. Biol. Chem.* 254:508–517.
29. Nesheim, M. E., J. B. Taswell, and K. G. Mann. 1979. The contribution of bovine factor V and factor Va to the activity of prothrombinase. *J. Biol. Chem.* 254:10952–10962.
30. Heldebrant, C. M., R. J. Butkowski, …, K. G. Mann. 1973. The activation of prothrombin. II. Partial reactions, physical and chemical characterization of the intermediates of activation. *J. Biol. Chem.* 248:7149–7163.
31. Griffith, M. J., C. M. Noyes, and F. C. Church. 1985. Reactive site peptide structural similarity between heparin cofactor II and antithrombin III. *J. Biol. Chem.* 260:2218–2225.
32. Kalb, E., S. Frey, and L. K. Tamm. 1992. Formation of supported planar bilayers by fusion of vesicles to supported phospholipid monolayers. *Biochim. Biophys. Acta.* 1103:307–316.
33. Tamm, L. K., and H. M. McConnell. 1985. Supported phospholipid bilayers. *Biophys. J.* 47:105–113.
34. Côté, H. C. F., L. Bajzar, …, M. E. Nesheim. 1997. Functional characterization of recombinant human meizothrombin and meizothrombin (desF1). Thrombomodulin-dependent activation of protein C and thrombin-activatable fibrinolysis inhibitor (TAFI), platelet aggregation, antithrombin-III inhibition. *J. Biol. Chem.* 272:6194–6200.
35. Jones, K. C., and K. G. Mann. 1994. A model for the tissue factor pathway to thrombin. II. A mathematical simulation. *J. Biol. Chem.* 269:23367–23373.
36. Doyle, M. F., and K. G. Mann. 1990. Multiple active forms of thrombin. IV. Relative activities of meizothrombins. *J. Biol. Chem.* 265:10693–10701.
37. Nesheim, M. E., S. Eid, and K. G. Mann. 1981. Assembly of the prothrombinase complex in the absence of prothrombin. *J. Biol. Chem.* 256:9874–9882.
38. Bird, R. B., W. E. Stewart, and E. N. Lightfoot. 2002. Transport Phenomena. John Wiley & Sons, New York.
39. Brummel, K. E., S. G. Paradis, …, K. G. Mann. 2002. Thrombin functions during tissue factor-induced blood coagulation. *Blood.* 100: 148–152.
40. Rosing, J., G. Tans, …, H. C. Hemker. 1980. The role of phospholipids and factor Va in the prothrombinase complex. *J. Biol. Chem.* 255: 274–283.
41. Reference deleted in proof.
42. Kung, C., E. Hayes, and K. G. Mann. 1994. A membrane-mediated catalytic event in prothrombin activation. *J. Biol. Chem.* 269:25838–25848.
43. Deiter, S. R., and G. M. Rodgers. 2004. Thrombosis and antithrombotic therapy. *In* Wintrobe's Clinical Hematology. J. P. Greer, J. Foerster, J. N. Lukens, G. M. Rodgers, F. Paraskevas, and B. Glader, editors. Williams & Wilkins, Philadelphia, PA. 1413–1758.
44. Virchow, R. 1998. Thrombosis and emboli. Vascular inflammation and septic infection. *In* Collected Essays on Medical Science [Thrombose und Embolie. Gefassentzundung und septische Infektion. *In* Gesammelte Abhandlungen zur wissenschlaflichen Medicin].. Von Meidinger & Sohn, Frankfurt am Main, Germany. 219–732.
45. Reference deleted in proof.
46. Reference deleted in proof.
47. Hockin, M. F., K. C. Jones, …, K. G. Mann. 2002. A model for the stoichiometric regulation of blood coagulation. *J. Biol. Chem.* 277:18322–18333.
48. Schoen, P., and T. Lindhout. 1987. The in situ inhibition of prothrombinase-formed human α-thrombin and meizothrombin(des F1) by antithrombin III and heparin. *J. Biol. Chem.* 262:11268–11274.
49. Bovill, E. G., R. P. Tracy, …, K. G. Mann. 1995. Evidence that meizothrombin is an intermediate product in the clotting of whole blood. *Arterioscler. Thromb. Vasc. Biol.* 15:754–758.
50. Lim, T. K., V. A. Bloomfield, and G. L. Nelsestuen. 1977. Structure of the prothrombin- and blood clotting factor X-membrane complexes. *Biochemistry.* 16:4177–4181.
51. Harmison, C. R., R. H. Landaburu, and W. H. Seegers. 1961. Some physicochemical properties of bovine thrombin. *J. Biol. Chem.* 236:1693–1696.